

## Experimental Studies on Multi-bladed S-shaped Vane type Rotor

Z. Afroz\*, M.Q. Islam\* and M. Ali\*

Received 15 May 2011; Accepted after revision 30 December 2011

### ABSTRACT

*The present research work studies the dynamic conditions of Multi bladed rotor at different Reynolds number. The investigation on wind loading and aerodynamic effects on the four, five and six bladed S-shaped vertical axis vane type rotor has been conducted with the help of an open circuit subsonic wind tunnel. For different bladed rotor the flow velocities were varied from 5m/s to 9m/s covering the Reynolds numbers up to  $1.35 \times 10^5$ . It was observed that by increasing the number of blades of rotor to the optimum limit considering all significant factors and at the same time by increasing its Reynolds number, the power output can be increased to its maximum level. It was also found that at higher Reynolds number the value of maximum torque co-efficient is slightly lower. However, at the same Reynolds number for rotor having higher number of blades the maximum value of torque coefficient is also higher which is very important for irrigation purpose. Finally, the nature of predicted dynamic characteristics has been analyzed by comparing with the existing research works. For comparison power coefficient versus tip speed ratio of the present measurement and previous researcher's works has been*

---

\* Department of ME, Bangladesh University of Engineering and Technology (BUET),  
Dhaka-1000, Bangladesh. Email: [zakia\\_afroz@yahoo.com](mailto:zakia_afroz@yahoo.com)

*plotted on the same graph. It is seen that there is a close correlation between the values predicted by the present method and those obtained from the existing research works and the nature of all compared curves are similar to previous measurements.*

*Keywords: Rotor, Dynamic characteristics, Multi-blade, Reynolds number.*

## **1 INTRODUCTION**

The utilization of wind energy is not a new technology but draws on the rediscovery of a long tradition of wind power technology. However, expected developments have not been achieved in wind driven machines to cope with the characteristics of wind turbines. Conventional machines are being used now a day even though they are not always suitable from the operational point of view. Arising from the increasing practical importance of wind turbine aerodynamics, there have been, over the past few decades, enormous increases in research works concerning laboratory simulations, full-scale measurements and more recently, numerical calculations and theoretical predictions of flows over a wide variety of vane type wind turbine. Bowden, G.J. and McAleese, S.A. [2] made some measurements on the Queensland optimum S-shaped rotor to examine the properties of isolated and coupled S-shaped rotor. Huda et al. [3] analyzed the performance of S-shaped rotor by placing a flat plate in front of the returning blade. Islam et al. [4] investigated Aerodynamic characteristics of a stationary Savonius rotor of two semi cylindrical blades. Islam et al. [5] investigated the aerodynamic forces acting on a stationary S-shaped rotor and made an attempt to predict the dynamic performance from these forces. Saha and Maity [6] experimented for augmenting the energy-harnessing effectiveness and finally, suggested that the use of the partially blocking wedge is highly desirable. Islam et al. [7] investigated the drag and torque coefficients of a stationary five bladed vane type rotor by measuring the pressure distribution on the blade surfaces at various rotor angles. Swamy and Fritzsche [8] investigated with the objective to improve the Darrieus type of motor.

This paper reports on the investigation on wind loading and aerodynamic effects on the four, five and six bladed S-shaped vertical axis vane type rotor conducted with the help of a subsonic wind tunnel together with the experimental set-up of the vane type rotor and a spring balance. This Vane type rotor of S-

shaped cross section is predominantly drag based, but also uses a certain amount of aerodynamic lift. Drag based vertical axis wind turbines have relatively higher starting torque and less rotational speed than their lift based counterparts. Furthermore, their power output to weight ratio is also less. Because of the low speed, these are generally considered unsuitable for producing electricity, although it is possible by selecting proper gear trains. Drag based windmills are useful for other applications such as grinding grain, pumping water and a small output of electricity. A major advantage of drag based vertical axis wind turbines lies in their self-starting capacity, unlike the Darrieus lift-based vertical axis wind turbines.

## 2 SET-UP OF THE EXPERIMENT

The experiment was carried out in the open circuit subsonic type 5.93 meter long wind tunnel with an outlet test section of (490 mm x 490 mm) cross-section and the rotor was positioned at the exit section of the wind tunnel. The rotors were made of PVC material. Both the top and bottom ends of the rotor were fitted with end caps. The whole rotor was fixed on an iron frame by using a shaft that was inserted into it and two ball bearings. A pulley was attached at one end of shaft. A strip whose one side was tied to a spring balance and other side to a load carrying plate was prepared for passing over that pulley. A radium sticker was attached to that side of shaft. The spring balance was attached to the iron frame. The whole experimental set-up is shown in **Fig.1**.

1. CONVERGING MOUTH ENTRY
2. PERSPEX SECTION
3. RECTANGULAR DIVERGING SECTION
4. FAN SECTION
5. BUTTERFLY SECTION
6. SILENCER WITH HONEYCOMB SECTION
7. DIVERGING SECTION
8. CONVERGING SECTION
9. RECTANGULAR SECTION
10. FLOW STRAIGHTNER SECTION
11. RECTANGULAR EXIT SECTION

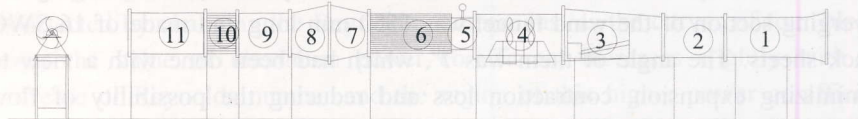


**Figure 1:** Schematic diagram of wind tunnel.

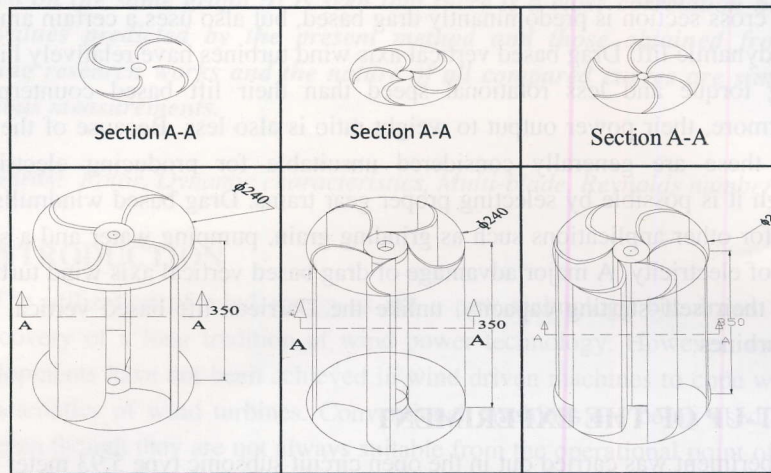


**Figure 2:** Cross-sectional and three dimensional views of four, five and six bladed rotor.

As can be seen from **Fig.1** the successive sections of the wind tunnel comprised of a converging entry, a Perspex section, a rectangular section, a fan section (two rotary axial flow fans), a butterfly valve section, a silencer with honey comb section, a diverging section, a converging section and an exit flow straightened section. The central longitudinal axis of the wind tunnel was maintained at a constant height from the floor. The converging mouth entry was incorporated into the system for easy entry of air into the tunnel and maintains uniform flow into the duct free from outside disturbances. In order to smooth the flow, the honeycomb was fixed near the outlet of the wind tunnel. The induced flow through the wind tunnel was produced by two-stage rotating axial flow fan of capacity  $18.16 \text{ m}^3/\text{s}$  at a head of  $152.4 \text{ mm}$  of water and  $1475 \text{ rpm}$  with each of the fans connected to a motor of  $2.25 \text{ kW}$  capacity and  $2900 \text{ rpm}$ . A butterfly valve as shown in **Fig.1** was used to control the wind speed. It was actuated by a screw thread mechanism placed behind the fan. A silencer was connected just after the butterfly valve for reduction of noise of the system. The converging and diverging section of the wind tunnel was  $1550 \text{ mm}$  long and made of 16 SWG black sheets. The angle of them was  $7^\circ$ , which had been done with a view to minimizing expansion, contraction loss and reducing the possibility of flow separation. Other three outlet square ( $610 \text{ mm}$  each) sections were used to make the flow straight and uniform. The cross-sectional and three dimensional views of four, five and six bladed S-shaped vane type rotors are shown in **Fig.2**.

### 3 RESULTS AND DISCUSSION

The variation of results for four, five and six bladed S-shaped vane type rotor in terms of power co-efficient versus tip speed ratio for increasing Reynolds number are shown in **Fig.3**, **Fig.4** and **Fig.5** respectively.

In **Figure 3** power coefficient versus tip speed ratio have been presented for 4 bladed S-shaped rotors at Reynolds numbers  $0.75 \times 10^5$ ,  $0.90 \times 10^5$ ,  $1.05 \times 10^5$ ,  $1.20 \times 10^5$  and  $1.35 \times 10^5$ . The variations of Reynolds number were made by varying the free steam velocity. For four bladed rotors at Reynolds number  $0.75 \times 10^5$  maximum power coefficient of 0.1398 occurs at tip speed ratio of 0.6836. For further loading step by step with the decrease in rotor r.p.m., tip speed ratio also decreases from 0.6836 to 0.3644. However, the value of power co-efficient starts falling as the tip speed ratio becomes lower than 0.6836 although so far it was at increasing condition. At Reynolds number of  $0.90 \times 10^5$  maximum power coefficient of 0.1411 occurs at tip speed ratio of 0.7037. From these two curves it is observed that the maximum power co-efficient is affected by changing the Reynolds number. For comparatively higher value of Reynolds number the value of maximum power co-efficient is slightly higher and it is shifted towards the higher values of tip speed ratios as the Reynolds number is increased. For Reynolds number of  $1.05 \times 10^5$ ,  $1.20 \times 10^5$  and  $1.35 \times 10^5$  the repetition of same event can be observed. At Reynolds numbers of  $1.05 \times 10^5$ ,  $1.20 \times 10^5$  and  $1.35 \times 10^5$  maximum power coefficients of 0.1433, 0.1453 and 0.1483 occur at tip speed ratios of 0.7434, 0.75 and 0.77 respectively.

In **Figure 4** for five bladed S-shaped rotor power co-efficient versus tip speed ratio have been presented at Reynolds numbers of  $0.75 \times 10^5$ ,  $0.90 \times 10^5$ ,  $1.05 \times 10^5$ ,  $1.20 \times 10^5$  and  $1.35 \times 10^5$ . For five bladed rotors at Reynolds number of  $0.75 \times 10^5$  maximum power coefficient of 0.1421 occurs at tip speed ratio of 0.5906. For further loading step by step with the decrease in tip speed ratio from 0.5906 to 0.2262 power co-efficient also decreases from 0.1421 to 0.0618. At Reynolds number of  $0.90 \times 10^5$  maximum power coefficient of 0.1464 occurs at tip speed ratio of 0.6493. For also five bladed rotor it is observed that just like previous Figure of Four bladed vane type rotor the maximum power co-efficient is affected by changing the Reynolds number. Just as the curves of four bladed rotor the value of maximum power co-efficient increases slightly with the increase of Reynolds number and the region of this higher power co-efficient move to the region of larger values of tip speed ratios. For Reynolds number  $1.05 \times 10^5$ ,  $1.20 \times 10^5$  and  $1.35 \times 10^5$  the repetition of same event can be observed. At Reynolds numbers of  $1.05 \times 10^5$ ,  $1.20 \times 10^5$  and  $1.35 \times 10^5$  maximum power

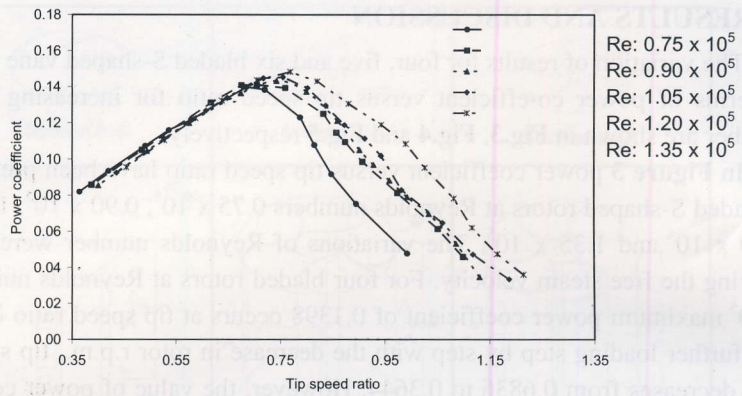


**Figure 3:** Comparisons of power coefficient vs. tip speed ratio for Four Bladed S-shaped Rotor at different Reynolds number.

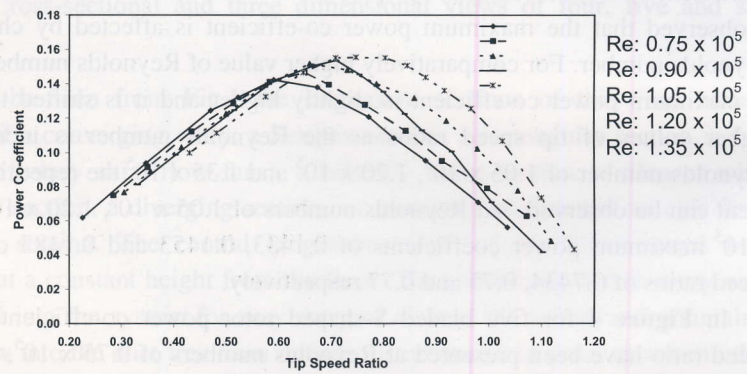


**Figure 4:** Comparisons of power coefficient vs. tip speed ratio for Five Bladed S-shaped Rotor at different Reynolds number.

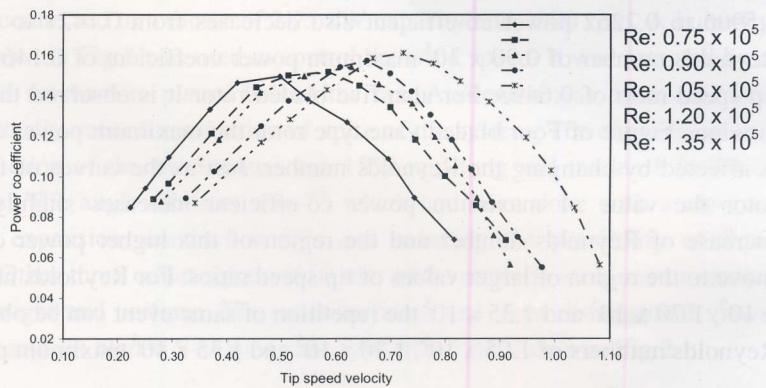


**Figure 5:** Comparisons of power coefficient vs. tip speed ratio for Six Bladed S-shaped Rotor at different Reynolds number.

coefficients of 0.1516, 0.1535 and 0.1553 occur at tip speed ratios of 0.6588, 0.71 and 0.7470 respectively.

In **Figure 5** for six bladed S-shaped vane type rotor power co-efficient versus tip speed ratio have been presented at Reynolds numbers of  $0.75 \times 10^5$ ,  $0.90 \times 10^5$ ,  $1.05 \times 10^5$ ,  $1.20 \times 10^5$  and  $1.35 \times 10^5$ . For six bladed rotor at Reynolds number of  $0.75 \times 10^5$  maximum power coefficient of 0.1497 occurs at tip speed ratio of 0.4976. For further loading step by step as the value of tip speed ratio decreases from 0.4976 to 0.2237 power co-efficient also decreases from 0.1497 to 0.0848. For Reynolds numbers of  $0.90 \times 10^5$ ,  $1.05 \times 10^5$ ,  $1.20 \times 10^5$  and  $1.35 \times 10^5$  maximum power coefficients of 0.1519, 0.1543, 0.1574 and 0.1611 occur at tip speed ratios of 0.5864, 0.6283, 0.6566 and 0.7233 respectively. Just as previous Figures of four and five bladed vane type rotors, for also six bladed rotor it is observed that the maximum power co-efficient is affected by changing the Reynolds number. For also six bladed rotor comparatively at higher values of Reynolds number the value of maximum power co-efficient is slightly higher and the region of this higher power co-efficient move to the region of larger values of tip speed ratios.

From these graphs (**Fig.3**, **Fig.4** and **Fig.5**) it is evident that with the increase of Reynolds number the maximum value of power coefficient also increases and it is shifted towards the higher values of tip speed ratios.

In **Figures 6-10** comparisons have been made among three different power co-efficient versus tip speed ratio curves of 4, 5 and 6 bladed rotor at different Reynolds number. In each figure a comparison has been made among different curves of power co-efficient versus tip speed ratio of four, five and six bladed rotor at a particular Reynolds number.

It can be seen from **Fig.6** that for four bladed rotor at Reynolds number  $0.75 \times 10^5$  maximum power coefficient of 0.1398 occurs at tip speed ratio of 0.6836. Whereas for 5 and 6 bladed rotors at the same Reynolds number maximum power coefficients of 0.1421 and 0.1497 occur at tip speed ratios of 0.5906 and 0.4976 respectively. From this graph it is evident that with the increase in number of blades the maximum value of power coefficient also increases and it is shifted towards the lower values of tip speed ratio.

In **Figures 7-10** the same thing can be observed. For 4, 5 and 6 bladed rotors at Reynolds number of  $0.90 \times 10^5$  maximum power coefficients of 0.1411, 0.1464 and 0.1519 occur at tip speed ratios of 0.7037, 0.6493 and 0.5864 respectively. Similarly, at Reynolds number  $1.05 \times 10^5$ ,  $1.20 \times 10^5$  and  $1.35 \times 10^5$  it can be observed that the value of maximum power co-efficient also becomes higher for

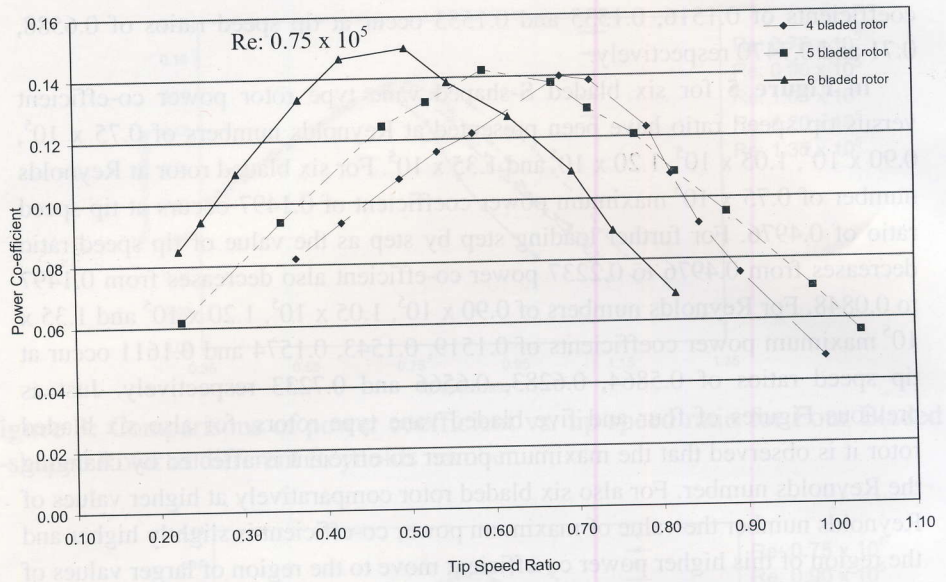


**Figure 6:** Comparisons of power coefficient versus tip speed ratio of 4, 5 and 6 bladed rotors at Reynolds number of  $0.75 \times 10^5$ .

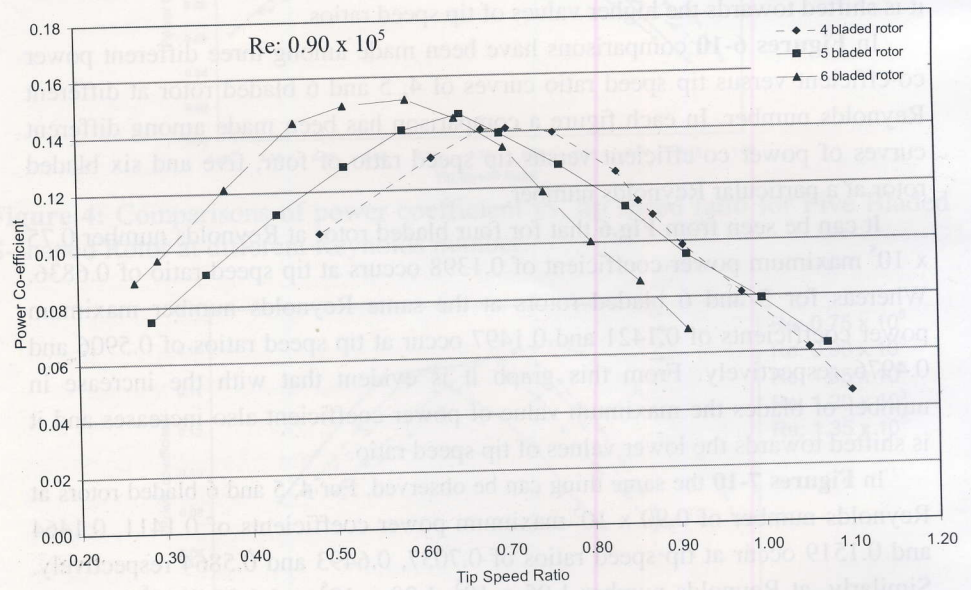


**Figure 7:** Comparisons of power coefficient versus tip speed ratio of 4, 5 and 6 bladed rotors at Reynolds number of  $0.90 \times 10^5$ .

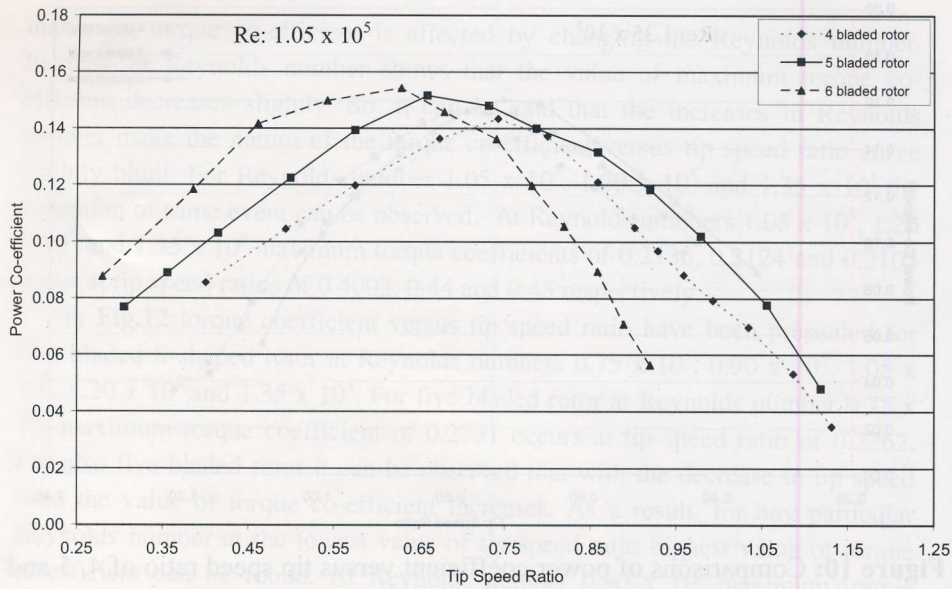


**Figure 8:** Comparisons of power coefficient versus tip speed ratio of 4, 5 and 6 bladed rotors at Reynolds number of  $1.05 \times 10^5$ .

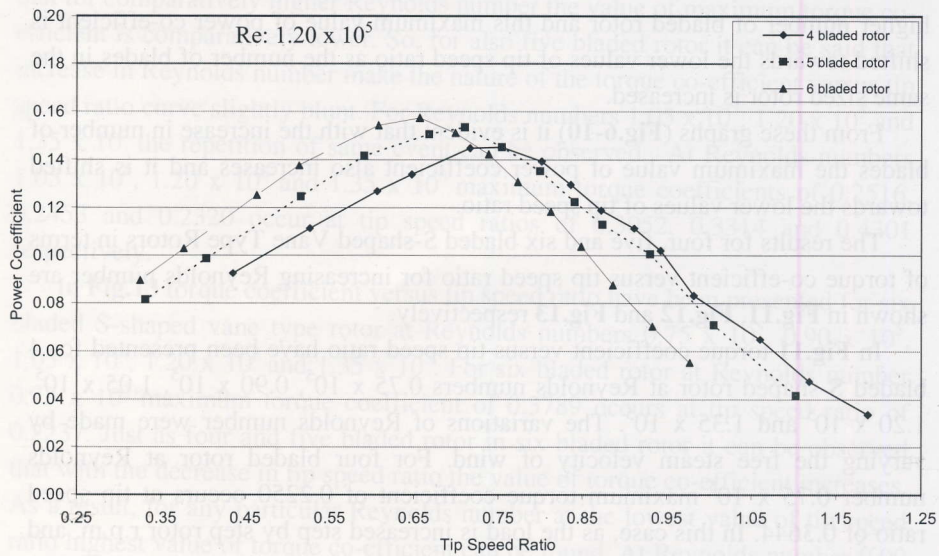


**Figure 9:** Comparisons of power coefficient versus tip speed ratio of 4, 5 and 6 bladed rotors at Reynolds number of  $1.20 \times 10^5$ .

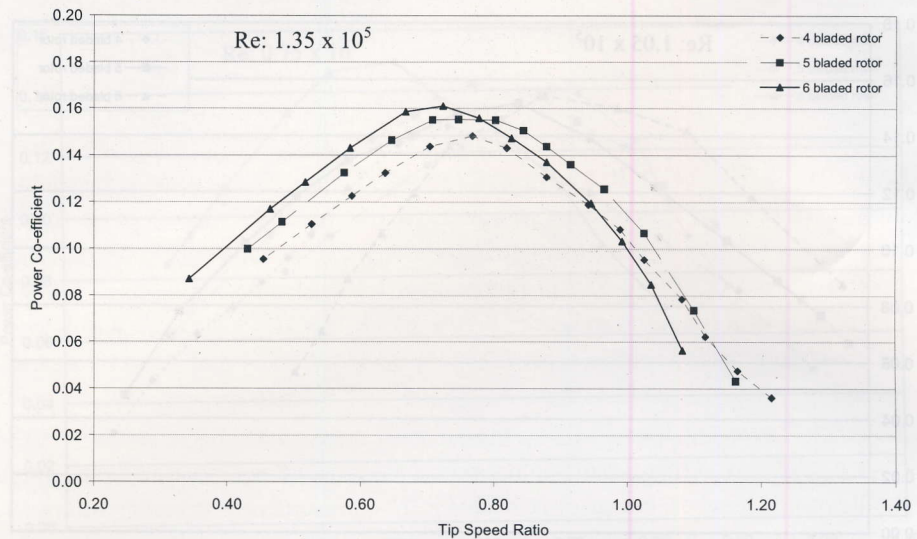


**Figure 10:** Comparisons of power coefficient versus tip speed ratio of 4, 5 and 6 bladed rotors at Reynolds number of  $1.35 \times 10^5$ .

**Figure 10:** Comparisons of power coefficient versus tip speed ratio of 4, 5 and 6 bladed rotors at Reynolds number of  $1.35 \times 10^5$ .

higher number of bladed rotor and this maximum value of power co-efficient is shifted towards the lower values of tip speed ratio as the number of blades in the same sized rotor is increased.

From these graphs (Fig.6-10) it is evident that with the increase in number of blades the maximum value of power coefficient also increases and it is shifted towards the lower values of tip speed ratio.

The results for four, five and six bladed S-shaped Vane Type Rotors in terms of torque co-efficient versus tip speed ratio for increasing Reynolds number are shown in Fig.11, Fig.12 and Fig.13 respectively.

In Fig.11 torque coefficient versus tip speed ratio have been presented for 4 bladed S-shaped rotor at Reynolds numbers  $0.75 \times 10^5$ ,  $0.90 \times 10^5$ ,  $1.05 \times 10^5$ ,  $1.20 \times 10^5$  and  $1.35 \times 10^5$ . The variations of Reynolds number were made by varying the free steam velocity of wind. For four bladed rotor at Reynolds number  $0.75 \times 10^5$  maximum torque coefficient of 0.2250 occurs at tip speed ratio of 0.3644. In this case, as the load is increased step by step rotor r.p.m. and tip speed ratio decreases accordingly. However, the value of torque co-efficient increases accordingly. This is why, for any particular Reynolds number at the lowest value of tip speed ratio highest value of torque co-efficient can be found. At Reynolds number of  $0.90 \times 10^5$  maximum torque coefficient of 0.2214 occurs at tip speed ratio of 0.3875. From these two curves it is observed that the

maximum torque co-efficient is affected by changing the Reynolds number. Increase of Reynolds number shows that the value of maximum torque co-efficient decreases slightly. So, it can be said that the increases in Reynolds number make the nature of the torque co-efficient versus tip speed ratio curve slightly blunt. For Reynolds number  $1.05 \times 10^5$ ,  $1.20 \times 10^5$  and  $1.35 \times 10^5$  the repetition of same event can be observed. At Reynolds numbers  $1.05 \times 10^5$ ,  $1.20 \times 10^5$  and  $1.35 \times 10^5$  maximum torque coefficients of 0.2136, 0.2124 and 0.2105 occur at tip speed ratios of 0.4003, 0.44 and 0.45 respectively.

In **Fig.12** torque coefficient versus tip speed ratio have been presented for five bladed S-shaped rotor at Reynolds numbers  $0.75 \times 10^5$ ,  $0.90 \times 10^5$ ,  $1.05 \times 10^5$ ,  $1.20 \times 10^5$  and  $1.35 \times 10^5$ . For five bladed rotor at Reynolds number  $0.75 \times 10^5$  maximum torque coefficient of 0.2731 occurs at tip speed ratio of 0.2262. For also five bladed rotor it can be observed that with the decrease in tip speed ratio the value of torque co-efficient increases. As a result, for any particular Reynolds number at the lowest value of tip speed ratio highest value of torque co-efficient can be found. At Reynolds number  $0.90 \times 10^5$  maximum torque coefficient of 0.2631 occurs at tip speed ratio of 0.2848. Just as four bladed rotor in also five bladed rotor it is observed that the maximum torque co-efficient is affected by changing the Reynolds number. From these two curves it can be said that for comparatively higher Reynolds number the value of maximum torque co-efficient is comparatively lower. So, for also five bladed rotor it can be said that increase in Reynolds number make the nature of the torque co-efficient versus tip speed ratio curve slightly blunt. For Reynolds numbers  $1.05 \times 10^5$ ,  $1.20 \times 10^5$  and  $1.35 \times 10^5$  the repetition of same event can be observed. At Reynolds numbers  $1.05 \times 10^5$ ,  $1.20 \times 10^5$  and  $1.35 \times 10^5$  maximum torque coefficients of 0.2516, 0.2453 and 0.2320 occur at tip speed ratios of 0.3052, 0.3314 and 0.4301 respectively.

In **Fig.13** torque coefficient versus tip speed ratio have been presented for six bladed S-shaped vane type rotor at Reynolds numbers  $0.75 \times 10^5$ ,  $0.90 \times 10^5$ ,  $1.05 \times 10^5$ ,  $1.20 \times 10^5$  and  $1.35 \times 10^5$ . For six bladed rotor at Reynolds number  $0.75 \times 10^5$  maximum torque coefficient of 0.3789 occurs at tip speed ratio of 0.2237. Just as four and five bladed rotor in six bladed rotor it can be observed that with the decrease in tip speed ratio the value of torque co-efficient increases. As a result, for any particular Reynolds number at the lowest value of tip speed ratio highest value of torque co-efficient can be found. At Reynolds number  $0.90 \times 10^5$  maximum torque coefficient of 0.3342 occurs at tip speed ratio of 0.2660. For also six bladed rotor it is seen that the values of torque co-efficient with

respect to different tip speed ratios are different for different Reynolds numbers. From these two curves it can be said that for higher Reynolds number the value of maximum torque co-efficient is lower. That means the increase in Reynolds number make the nature of the torque co-efficient versus tip speed ratio curve slightly blunt. For Reynolds numbers  $1.05 \times 10^5$ ,  $1.20 \times 10^5$  and  $1.35 \times 10^5$  the repetition of same event can be observed. At Reynolds numbers  $1.05 \times 10^5$ ,  $1.20 \times 10^5$  and  $1.35 \times 10^5$  maximum torque coefficients of 0.3130, 0.2749 and 0.2543 occur at tip speed ratios of 0.2801, 0.3252 and 0.3421 respectively.

From these graphs (**Fig.11-13**) it is evident that for higher Reynolds number the maximum value of torque coefficient is lower and it is shifted towards the higher values of tip speed ratio.

In **Fig.14-18** comparisons have been made among the curves of torque co-efficient versus tip speed ratio of multi-bladed S-shaped rotor at different Reynolds numbers.

In **Fig.14** it can be observed that for four bladed rotor at Reynolds number  $0.75 \times 10^5$  maximum torque coefficient of 0.2250 occurs at tip speed ratio of 0.3644. Whereas for 5 and 6 bladed rotors at the same Reynolds number maximum torque coefficients of 0.2731 and 0.3789 occur at tip speed ratios of 0.2262 and 0.2237 respectively. This point is important for driving the irrigation pump especially positive displacement pump which needs higher starting torque. From this graph it is evident that for rotor having higher number of blades the maximum value of torque coefficient is also higher and it is shifted towards the lower values of tip speed ratio. That means, the increases in number of blades make the nature of torque co-efficient versus tip speed ratio curve sharper.

In **Fig.15-18** the same thing can be observed. For 4, 5 and 6 bladed rotors at Reynolds number  $0.90 \times 10^5$  maximum torque coefficients of 0.2214, 0.2631 and 0.3342 occur at tip speed ratios of 0.3875, 0.2848 and 0.2660 respectively. Similarly, at Reynolds number  $1.05 \times 10^5$ ,  $1.20 \times 10^5$  and  $1.35 \times 10^5$  it can be observed that the value of maximum torque co-efficient becomes higher for higher number of bladed rotor and this maximum value of torque co-efficient is shifted towards the lower value of tip speed ratio as the number of blades in the same sized rotor is increased.

From these graphs (**Fig.14-18**) it is evident that for rotor having higher number of blades the maximum value of torque coefficient is also higher and it is shifted towards the lower values of tip speed ratio.

In **Fig.19-24** the nature of predicted dynamic aerodynamic characteristics have been analyzed by comparing them with existing research works of Huda et al. [3], Littler [11], Bowden et al. [2].

In **Fig.19** the nature of predicted power co-efficient versus tip speed ratio curves for free stream velocities of 6 and 7 m/s has been compared with the same curve of Huda et al. [3] (without attaching deflecting plate in the experimental setup) for free stream velocity of 6.5 m/s. From this figure it is seen that there is a close correlation between the values predicted by the present method and those predicted by Huda et al. [3]. In **Fig.19** the nature of all curves are same although because of rotor swept area, blade number, its thickness and shape the curve predicted by Huda et al. is slightly oversize. For the same reason the values of torque co-efficient with respect to tip speed ratio in the curve of Huda et al. of **Fig.20** are slightly higher. However the nature of all curves is almost same. Similarly, in **Fig.21** and **Fig.22** the nature of the curves of power co-efficient versus tip speed ratio and torque co-efficient versus tip speed ratio for the present thesis and for the research works of Huda et al. is almost same.

Similarly in **Fig.23** and **Fig.24** the variation of results predicted from present thesis for four bladed S-shaped vane type rotor in terms of power co-efficient versus tip speed ratio at different free stream velocities are compared with the existing research works that coincide with this thesis work. From these figures it is seen that there is a close correlation between the values predicted by the present method and those obtained from the existing research works of Littler [11] and Bowden et al. [2]. However, because of the variation in number of blades, free stream velocities, rotor swept area, shape of the blade, its thickness

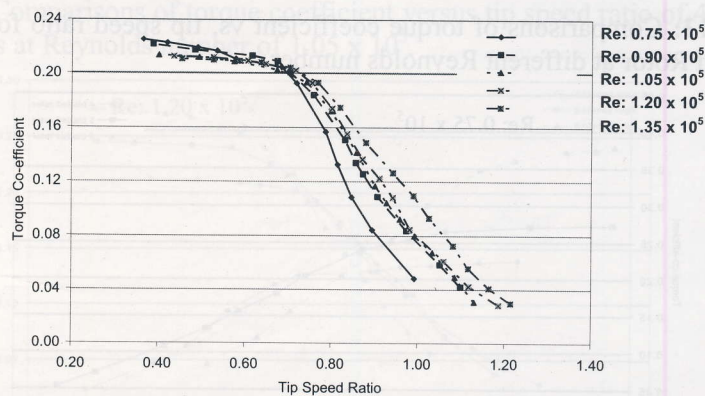


**Figure 11:** Comparisons of torque coefficient vs. tip speed ratio for Four Bladed S-shaped Rotor at different Reynolds number.

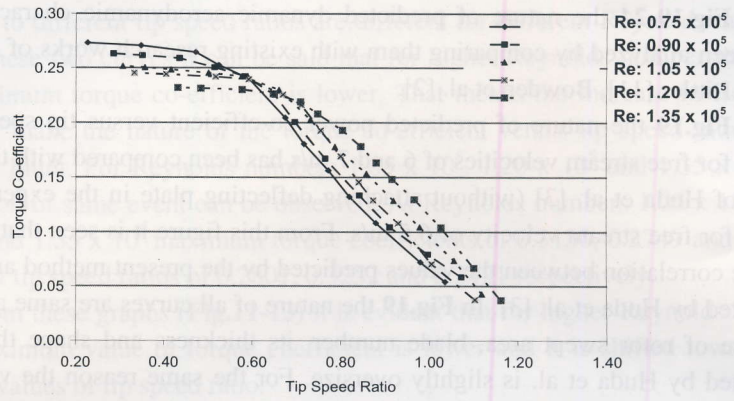


**Figure 12:** Comparisons of torque coefficient vs. tip speed ratio for Five Bladed S-shaped Rotor at different Reynolds number.

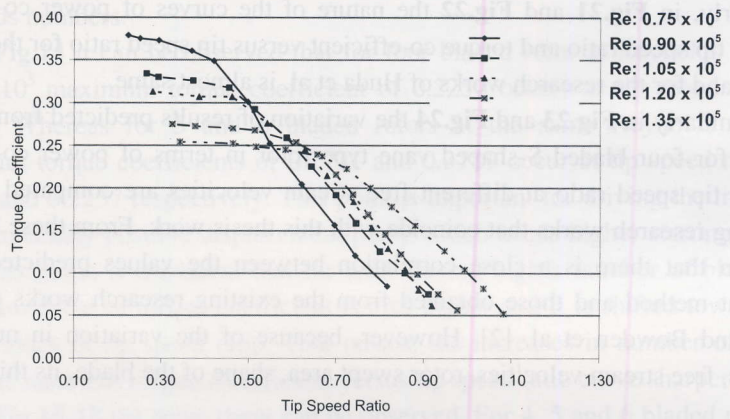


**Figure 13:** Comparisons of torque coefficient vs. tip speed ratio for Six Bladed S-shaped Rotor at different Reynolds number.

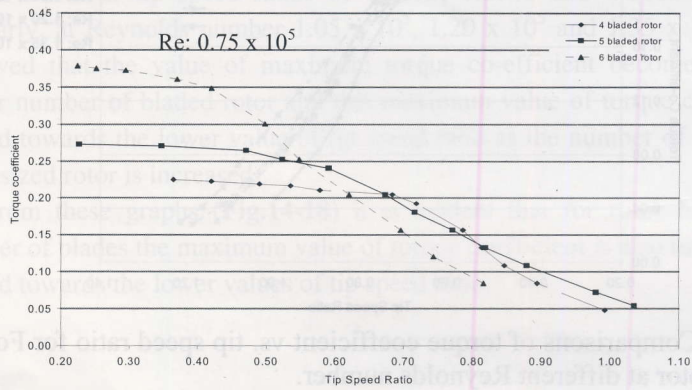


**Figure 14:** Comparisons of torque coefficient versus tip speed ratio of 4, 5 and 6 bladed rotors at Reynolds number of  $0.75 \times 10^5$ .

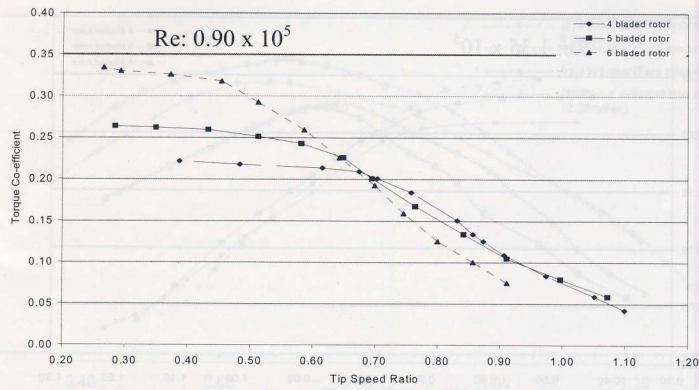


**Figure 15:** Comparisons of torque coefficient versus tip speed ratio of 4, 5 and 6 bladed rotors at Reynolds number of  $0.90 \times 10^5$ .

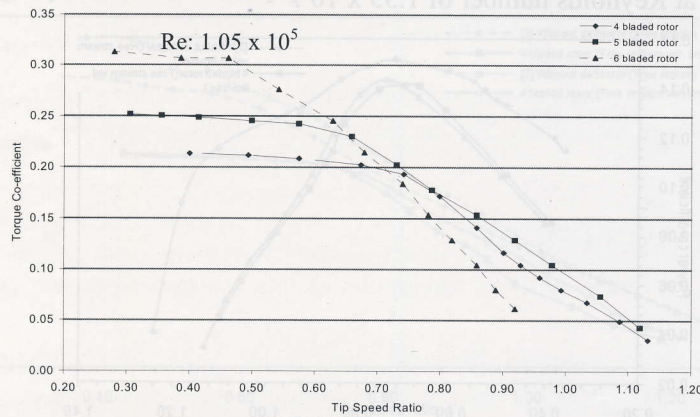


**Figure 16:** Comparisons of torque coefficient versus tip speed ratio of 4, 5 and 6 bladed rotors at Reynolds number of  $1.05 \times 10^5$ .

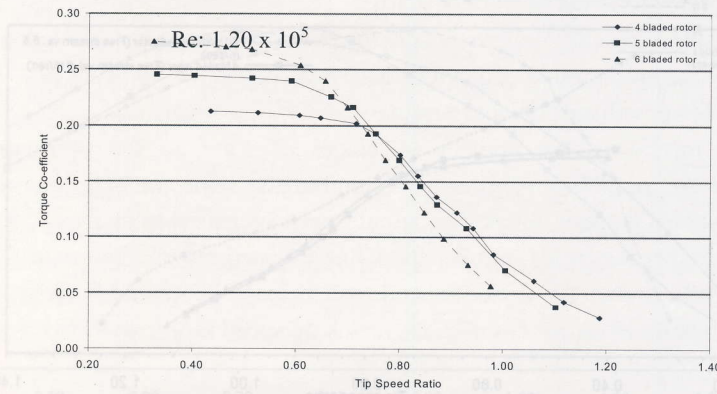


**Figure 17:** Comparisons of torque coefficient versus tip speed ratio of 4, 5 and 6 bladed rotors at Reynolds number of  $1.20 \times 10^5$ .

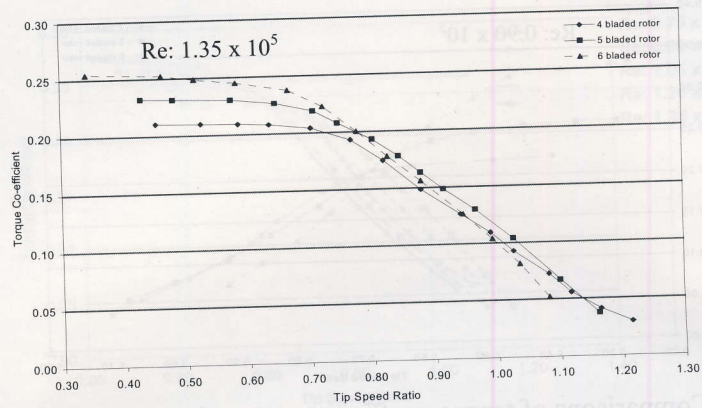


**Figure 18:** Comparisons of torque coefficient versus tip speed ratio of 4, 5 and 6 bladed rotors at Reynolds number of  $1.35 \times 10^5$ .

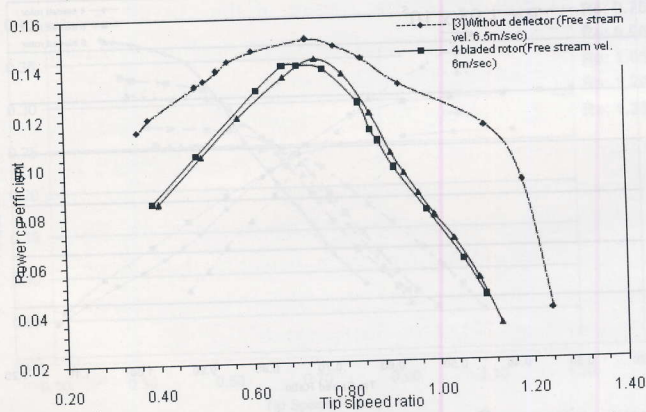


**Figure 19:** Comparisons of power coefficient versus tip speed ratio of present and existing experimental results [3].

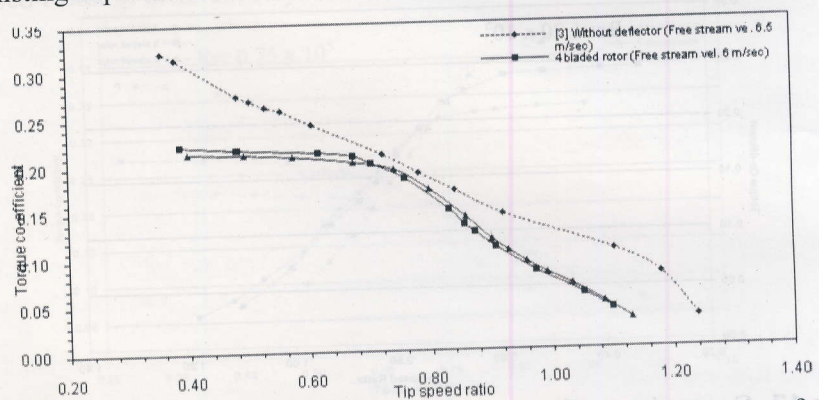


**Figure 20:** Comparisons of torque coefficient versus tip speed ratio of present and existing experimental results [3].

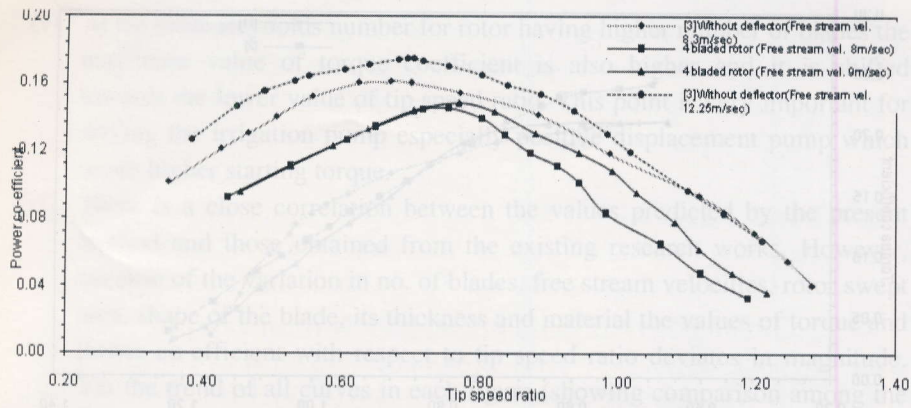


**Figure 21:** Comparisons of power coefficient versus tip speed ratio of present and existing experimental results [3].

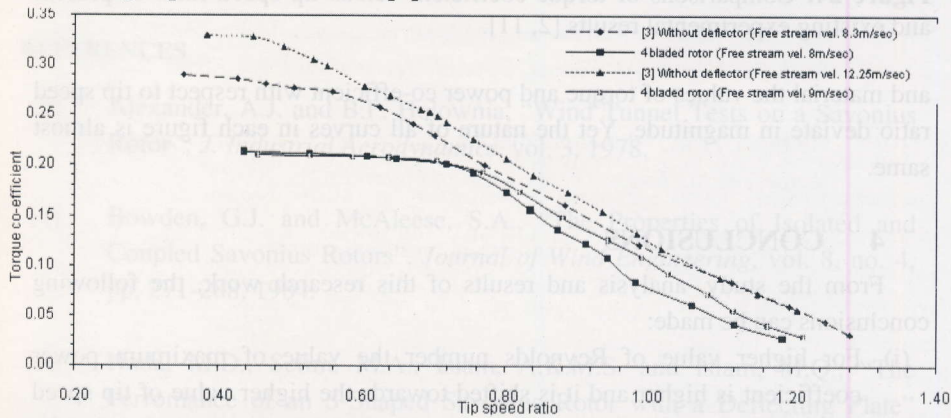


**Figure 22:** Comparisons of torque coefficient versus tip speed ratio of present and existing experimental results [3].

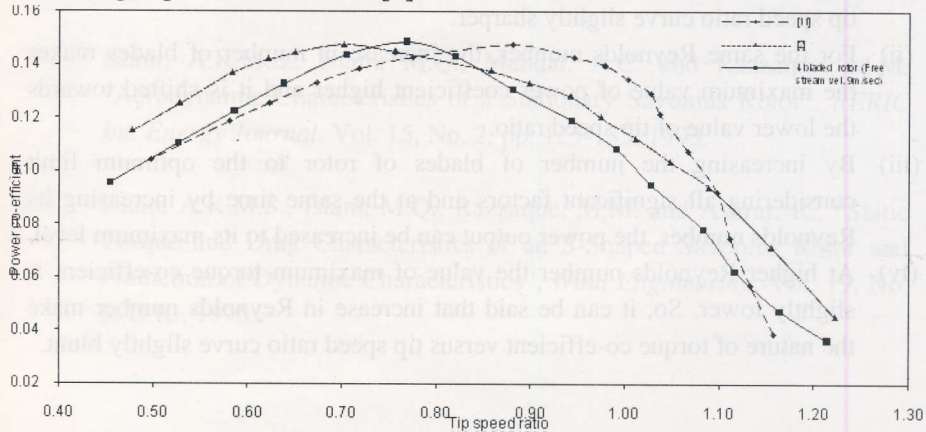


**Figure 23:** Comparisons of power coefficient versus tip speed ratio of present and existing experimental results [2, 11].

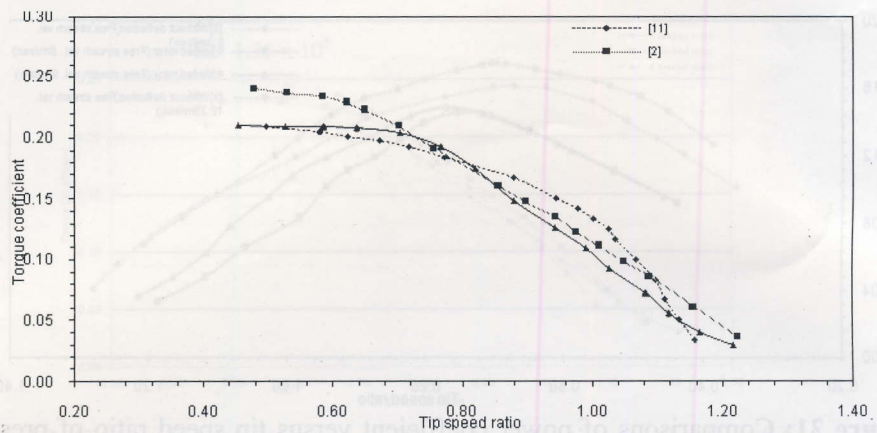


**Figure 24:** Comparisons of torque coefficient versus tip speed ratio of present and existing experimental results [2, 11].

and material the values of torque and power co-efficient with respect to tip speed ratio deviate in magnitude. Yet the nature of all curves in each figure is almost same.

#### 4 CONCLUSIONS

From the study, analysis and results of this research work, the following conclusions can be made:

- (i) For higher value of Reynolds number the value of maximum power coefficient is higher and it is shifted towards the higher value of tip speed ratio as the Reynolds number is increased. So, it can be concluded that the increase of Reynolds number make the nature of power co-efficient versus tip speed ratio curve slightly sharper.
- (ii) For the same Reynolds number, the increase in number of blades makes the maximum value of power coefficient higher and it is shifted towards the lower value of tip speed ratio.
- (iii) By increasing the number of blades of rotor to the optimum limit considering all significant factors and at the same time by increasing its Reynolds number, the power output can be increased to its maximum level.
- (iv) At higher Reynolds number the value of maximum torque co-efficient is slightly lower. So, it can be said that increase in Reynolds number make the nature of torque co-efficient versus tip speed ratio curve slightly blunt.

- (v) At the same Reynolds number for rotor having higher number of blades the maximum value of torque coefficient is also higher and it is shifted towards the lower value of tip speed ratio. This point is very important for driving the irrigation pump especially positive displacement pump which needs higher starting torque.
- (vi) There is a close correlation between the values predicted by the present method and those obtained from the existing research works. However, because of the variation in no. of blades, free stream velocities, rotor swept area, shape of the blade, its thickness and material the values of torque and power co-efficient with respect to tip speed ratio deviates in magnitude. Yet the trend of all curves in each figure (showing comparison among the trend of predicted dynamic aerodynamic characteristics and similar research works) is same.

#### REFERENCES

- [1] Alexander, A.J. and B.P. Holownia, "Wind Tunnel Tests on a Savonius Rotor", *J. Industrial Aerodynamics*, vol. 3, 1978.
- [2] Bowden, G.J. and McAleese, S.A., "The Properties of Isolated and Coupled Savonius Rotors", *Journal of Wind Engineering*, vol. 8, no. 4, pp. 271-288, 1984.
- [3] Huda, M.D., Selim, M.A., Islam, A.K.M.S. and Islam, M.Q., "The Performance of an S-Shaped Savonius Rotor with a Deflecting Plate" *RERIC International Energy Journal*: Vol. 14, No. 1, pp. 25-32, June 1992.
- [4] Islam, A.K.M.S., Islam, M.Q., Mandal, A.C. and Razzaque, M.M. "Aerodynamic Characteristics of a Stationary Savonius Rotor", *RERIC Int. Energy Journal*, Vol. 15, No. 2, pp. 125-135, 1993.
- [5] Islam, A.K.M.S., Islam, M.Q., Razzaque, M.M. and Ashraf, R., "Static Torque and Drag Characteristics of an S-Shaped Savonius Rotor and Prediction of Dynamic Characteristics", *Wind Engineering*, Vol. 19, No. 6, U.K., 1995.

- [6] Saha, U.K. and Maity, D., "Optimum Design Configuration of Savonius Rotor through Wind Tunnel Experiments", *Journal of Wind Engineering and Industrial Aerodynamics*, Volume 96, Issues 8-9, Pages 1359-1375, August-September 2008.
- [7] Kamal, F.M. and Islam, M.Q., "Aerodynamic Characteristics of a Stationary Five Bladed Vertical Axis Vane Type Wind Turbine" *Journal of Mechanical Engineering*, Vol. ME39, No. 2, IEB, December 2008.
- [8] Swamy, N.V.C. and Fritzsche, A.A., "Aerodynamic Studies on Vertical Axis Wind Turbine", *International Symposium on Wind Energy Systems, Cambridge, England, September 7-9, 1976*.
- [9] Rahman, M., "Aerodynamic Characteristics of a Three Bladed Savonius Rotor", *M.Sc. Engg. Thesis, Dept of Mechanical Engg., BUET, 2000*.
- [10] Bhuiyan, H. K., "Aerodynamic Characteristics of a Four Bladed Savonius Rotor", *M.Sc. Engg. Thesis, Dept of Mech. Engg., BUET, 2003*.
- [11] Littler, R.D., "Further Theoretical and Experimental Investigation of the Savonius Rotor", *B.E. Thesis, University of Queensland, 1975*.

## Experimental and Numerical investigation of Shock/Turbulence interaction by Hot-wire Technique

Mohammad Ali Jinnah\*

Received 14 May 2011; Accepted after revision 30 December 2011

### ABSTRACT

*In the present paper, an experimental investigation has been carried out to observe the amplification of turbulence intensity after shock/turbulence interaction by hot-wire technique. The hot wires are installed in the wake of the turbulent grids to measure the turbulence fluctuations before and after the reflected shock wave interaction with the turbulent field. Due to different grid plates, different strengths of turbulent fields are found behind the transmitted shock wave. It is observed that the turbulence fluctuations for less open area of the grid plate are higher than the turbulence fluctuations for more open area of the grid plate. Numerical simulations are also conducted on the experimental results where grid plate of 49.5 % open area is used. It is observed that the average longitudinal velocity line for the experimental velocity data simulate with numerical results properly and in some places, 5-7 % deviations are observed with numerical results. All the simulation results indicate that the present code with turbulence model is working properly for its initial conditions. The wall pressure fluctuations are also measured experimentally and substantial amplification of pressure fluctuations is observed after the shock/turbulence interaction. The rate of dissipation of*

---

\* Mechanical and Chemical Engineering Department, Islamic University of Technology (IUT), Board Bazar, Gazipur-1704, Bangladesh. Email: [jinnah@iut-dhaka.edu](mailto:jinnah@iut-dhaka.edu)